

## LASER $\mu$ -RAMAN INVESTIGATION OF GREEK BAUXITES FROM THE PARNASSOS-GHIONA ACTIVE MINING AREA

Gamaletsos P.<sup>1</sup>, Godelitsas A.<sup>1</sup>, Chatzitheodoridis E.<sup>2</sup>, and Kostopoulos D.<sup>1</sup>

<sup>1</sup> National and Kapodistrian University of Athens, Faculty of Geology and Geoenvironment,  
platon\_gk@geol.uoa.gr, agodel@geol.uoa.gr, dikostop@geol.uoa.gr

<sup>2</sup> National Technical University of Athens, School of Mining and Metallurgical Engineering,  
eliasch@central.ntua.gr

### Abstract

*Bauxite samples collected with permission from currently active mining areas in the Parnassos-Ghiona Mts district were studied using both conventional (optical microscopy and powder XRD) and, for the first time in the literature, micro-scale advanced non-destructive spectroscopic techniques, in particular Laser  $\mu$ -Raman. The results showed that the different bauxite types (diasporic or boehmitic) can easily be identified regardless of sample type (porous white-grey or massive red-brown) by recording spectra in the low-wavenumber region ( $250\text{ cm}^{-1} - 600\text{ cm}^{-1}$ ) where distinct bands of the natural AlOOH polymorphs are easily discernible ( $448\text{ cm}^{-1}$  for diasporic and  $362\text{ cm}^{-1}$  for boehmitic). The method described herein could equally be applied in the laboratory as well as in-situ at the mines for quick and accurate phase determination, in order to bypass the laborious and time-consuming indirect bulk techniques (such as XRD) routinely used to this date.*

**Key words:** Raman, Diasporic, Boehmitic, Bauxite, Greece.

### Περίληψη

Δείγματα βωξίτη τα οποία αποκτήθηκαν από εταιρείες που εμφανίζουν ενεργή μεταλλευτική δραστηριότητα στην περιοχή Παρνασσού-Γκιώνας χαρακτηρίστηκαν αρχικά με τη χρήση συμβατικών μεθόδων (οπτικό μικροσκόπιο, περίθλαση ακτίνων X) και στη συνέχεια μελετήθηκαν χρησιμοποιώντας, για πρώτη φορά στη διεθνή βιβλιογραφία, προηγμένες μή-καταστροφικές φασματοσκοπικές τεχνικές σε μικροκλίμακα (Laser  $\mu$ -Raman). Τα αποτελέσματα της παρούσας μελέτης έδειξαν πως ο τύπος του βωξίτη (διασπορικός ή μπειμιτικός) μπορεί εύκολα να προσδιοριστεί, ανεξάρτητα από το είδος του δείγματος (πορώδες λευκό-τεφρό ή και συμπαγές ερυθρό-φαιό), μέσω της καταγραφής του φάσματός του στην περιοχή χαμηλών ενεργειών ( $250\text{ cm}^{-1} - 600\text{ cm}^{-1}$ ) όπου και είναι ευδιάκριτες συγκεκριμένες Raman ταινίες των πολύμορφων του AlOOH ( $448\text{ cm}^{-1}$  για το διάσπορο και  $362\text{ cm}^{-1}$  για τον μπειμιτή). Η παραπάνω μικρο-μέθοδος θα μπορούσε να εφαρμοσθεί για τον άμεσο προσδιορισμό των ορυκτολογικών φάσεων τόσο στο εργαστήριο όσο και επιτόπου στα μεταλλεία, έτσι ώστε να αποφευχθούν έμμεσες και χρονοβόρες ολικές τεχνικές οι οποίες χρησιμοποιούνται έως και σήμερα (όπως π.χ. η περίθλαση ακτίνων X).

**Λέξεις κλειδιά:** Φασματοσκοπία, Διάσπορο, Μπειμιτής, Αιματίτης, Ανατάσης.

# 1. Introduction

In 2005, Greece was the twelfth bauxite producer in the world with a total production of  $2.2 \times 10^6$  tonnes (USGS – Mineral Commodity Summaries, January 2006). The bauxite reserves in Greece are estimated to be  $600 \times 10^6$  tonnes. It is now established that the Greek mining industry controls the most significant bauxite reserves in the EU (USGS – 2005 Minerals Yearbook). The overall production is mainly related to exploitation of bauxite deposits situated within the Parnassos-Ghiona geotectonic zone (central Greece) by three mining companies (Aluminium de Grèce S.A., S&B Industrial Minerals S.A., Elmin S.A.). Almost 72 % of the current Greek aluminium market is covered by domestic production (USGS – 2005 Minerals Yearbook). Most of the raw material is processed by Aluminium de Grèce at its metallurgical plant at Antikyra, Corinthiakos gulf, for the production of alumina and metallic aluminium to be used in industry and constructions. The remainder of the raw bauxite and associated metallurgical products are exported generating an annual income of ~25 and ~165 million € respectively, according to Greek Mining Enterprises Association.

Numerous geological studies have been published about the Parnassos-Ghiona allochthonous karst-type bauxite deposits (Aronis 1955, Papastamatiou 1960, Papastamatiou 1964, Bárdossy and Mack 1967, Nia 1971, Valeton, 1972, Maksimović and Papastamatiou 1973, Papastavrou 1974, Mack and Petrascheck 1978, Nicolas and Bildgen 1979, Combes *et al.* 1981, Bárdossy 1982, Biermann 1983, Combes and Andreou 1983, Arp 1985, Papastavrou 1986, Valeton *et al.* 1987, Petrascheck 1989, Valeton 1991, Vgenopoulos and Daskalakis 1991, Economopoulos and Vgenopoulos 1998). These ores are hosted within Mesozoic carbonate formations (Fig. 1). The Parnassos-Ghiona geotectonic zone is characterised by nearly continuous sedimentation of epicontinental reef-like carbonates from the Upper Triassic to the Upper Cretaceous (Valeton *et al.* 1987). In this carbonate sequence three bauxite horizons (from bottom to top: B<sub>1</sub>, B<sub>2</sub> and B<sub>3</sub>) can be distinguished and they were caused by epirogenic emersion phases and formation of coastal karst reliefs (Valeton *et al.* 1987, Petrascheck 1989). Horizon B<sub>1</sub> is hosted in the calcareous Middle-Upper Jurassic units, horizon B<sub>2</sub> in the calcareous Upper/Jurassic – Lower Cretaceous units (Tithonian and Neokomian respectively), whereas horizon B<sub>3</sub> is hosted in the calcareous Upper Cretaceous units (Cenomanian – Turonian).

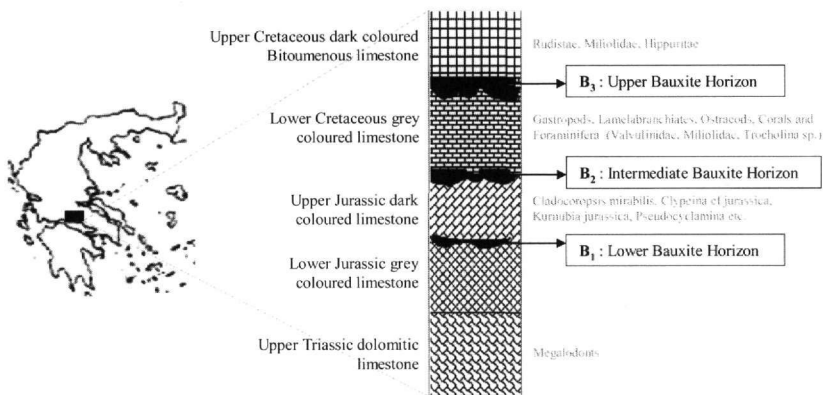


**Figure 1 - Stratigraphic position of bauxite horizons B<sub>1</sub>, B<sub>2</sub> and B<sub>3</sub> intercalated with shallow-water Jurassic to Cretaceous limestones of the Parnassos-Ghiona zone (modified, from Valeton *et al.* 1987)**

The main mineralogical and geochemical characteristics of the Parnassos-Ghiona bauxites have been described by several authors using conventional methods such as optical microscopy, SEM-EPMA, XRD, XRF, Fire-Assay/AAS/ICP and TGA/DTA (Kiskyras 1960, Nia 1968, Bárdossy and Pantó 1971, Ochsenkühn and Parissakis 1977, Augustithis *et al.* 1978, Combes 1979, Biermann 1983, Arp 1985, Paspaliaris 1985, Kritsotakis *et al.* 1986, Papastavrou and Perdikatsis

1987, Economopoulou-Kyriakopoulou 1991, Laskou 1991, Perdikatsis 1992, Ochsenkühn-Petropoulou and Ochsenkühn 1995, Laskou 2001, Laskou and Andreou 2003, Laskou 2005, Solymár *et al.* 2005, Laskou and Economou 2006). More detailed characterization techniques, and particularly TEM and INAA, have also been used (Bárdossy and Mack 1967, Laskou and Economou 1991, Ochsenkühn-Petropoulou and Ochsenkühn 1995, Ochsenkühn *et al.* 1995, Lymperopoulou 1996, Ochsenkühn *et al.* 2002). It is evident that the only non-bulk (micro- and nano-scale) instrumental methodology used so far, for the study of Parnassos-Ghiona bauxites, concerns some electron microscopy techniques (TEM and SEM-EPMA). Here, we present, for the first time in the literature, the application of micro-scale, non-destructive, advanced spectroscopic techniques such as laser  $\mu$ -Raman in the characterisation of typical bauxite samples from the Parnassos-Ghiona active mining area. We demonstrate that this method can equally be applied in the laboratory as well as *in-situ* at the mines (e.g. by using portable spectrometers) for quick and accurate phase determination, thus bypassing laborious and time-consuming indirect bulk techniques (such as XRD) routinely used to this date.

## 2. Materials and Methods

The investigated bauxite samples were collected during the period March 2006 – September 2006 from mining sites (Fig. 2) of the three Greek companies (Aluminium de Grèce S.A. indicated as “ALM”, Elmin S.A. indicated as “ELM” and S&B Industrial Minerals S.A. indicated as “SAB”, Table 1) exploiting bauxite in the Parnassos-Ghiona area (central Greece).

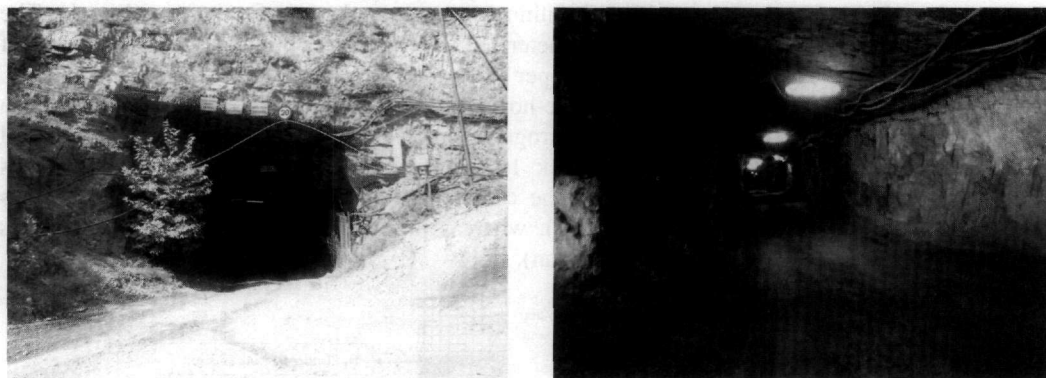


**Figure 2 – Bauxite underground works of Aluminium de Grèce at Pera-Lakkos site, Parnassos-Ghiona area**

The present investigation is focused on the analysis of bauxite samples from the 2<sup>nd</sup> (intermediate) and the 3<sup>rd</sup> (upper) bauxite horizon (Fig. 1, Table 1). All bauxites samples (both white-grey and red-brown) were initially investigated in polished-thin sections using transmitted and reflected light optical microscopy. The mineralogical composition was also examined using powder X-ray diffraction (XRD) on a Siemens D5005 (Bruker AXS) diffractometer using  $\text{CuK}\alpha$ -radiation. The Laser  $\mu$ -Raman spectra were obtained on the polished-thin sections using a Renishaw Ramascope RM 1000 equipment with a HeNe laser at 633 nm, a spectrometer with a grating of 1800 lines/mm, and a CCD Peltier-cooled detector. The laser beam diameter was adjusted depending on resolution requirements. In any case its maximum energy did not exceed 4 mW.

## 3. Results and discussion

The microscopic and XRD studies have shown that the major mineral phases in the investigated bauxite samples from the Parnassos-Ghiona deposits are the two common  $\text{AlOOH}$  polymorphs diaspore and boehmite, the typical  $\text{Fe}^{\text{III}}$  oxide and oxyhydroxide hematite and goethite, and the  $\text{TiO}_2$  polymorph anatase. Iron sulphides (such as pyrite) are frequently present. Microscopic

images (reflected light) of the most common in appearance (red-brown diasporic) bauxite samples are presented in Figure 3. Patches and veins of metallic minerals consisting of iron oxides and sulphides (lighter areas) are included in diasporic matrix (darker areas containing also pisoliths). Most of the characteristic bauxitic pisoliths contain both diaspore and finely dispersed hematite.

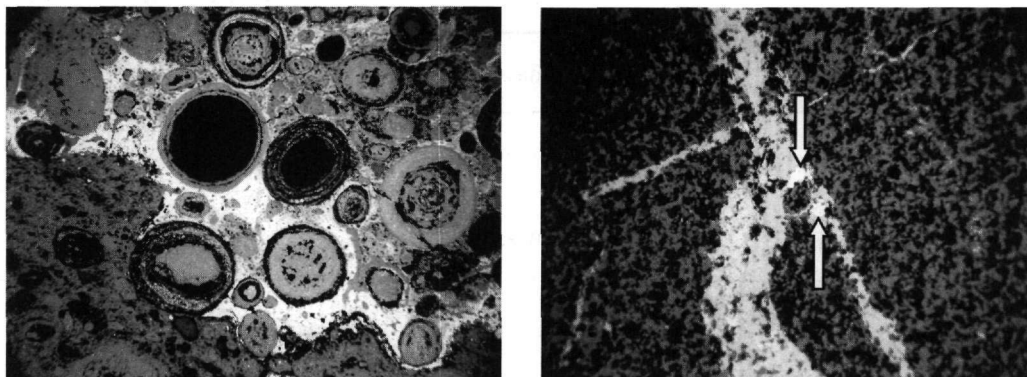


**Figure 3 – Representative microscopic images ( $\times 100$  and  $\times 200$ ) from typical red-brown diasporic bauxite samples using reflected light (lighter areas = Fe-oxides, arrows = sulphides)**

Typical XRD patterns of diasporic and boehmitic samples are shown in Figure 4 whereas the complete data are included in Table 1. It should be emphasized that the diasporic bauxite appears both in the form of porous white-grey (high quality) and red-brown samples, while boehmitic bauxite only in the form of massive red-brown samples.

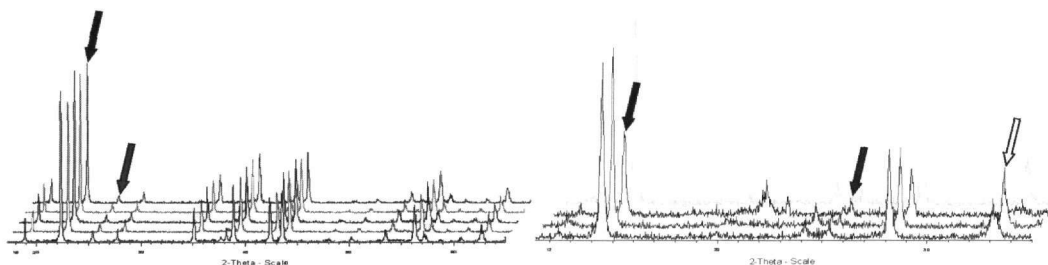


**Figure 4 – Powder XRD patterns of white-grey diasporic and red-brown boehmitic bauxite samples. In the first case the diaspore and anatase strongest reflections at 22.26 (3.99) and 25.35 (3.51)  $2\theta$  ( $d$  in Å) are indicated by black and grey arrows respectively, whereas in the second case boehmite, anatase and hematite strongest reflections at 14.48 (6.11), 25.35 (3.51) and 33.27 (2.69)  $2\theta$  ( $d$  in Å) are indicated by black, grey and white arrows respectively**

Conventional chemical methods are not recommended to characterize  $\text{AlOOH}$  polymorphs in bauxite samples. Thus powder XRD is fundamentally used in laboratory conditions. However it is rather difficult to use XRD for *in-situ* measurements in the field and in underground mining areas because portable XRD equipments are not greatly commercialized up to now. Therefore, it is important to suggest convenient spectroscopic methods, such as Laser  $\mu$ -Raman, which can be easily used for phase determination in any case. The instrument is a bench system capable of confocal imaging with high spectral and spatial resolution. Representative Laser  $\mu$ -Raman spectra of diasporic bauxite samples investigated during the present study (both white-grey and red-brown), together with standard Raman spectra from the Mineral Spectroscopy Server of CalTech (© Prof. G. Rossman 2006), are shown in Fig. 6. It should be noted that the spectra were obtained by focusing the laser beam on the diasporic matrix away from microscopically detectable metallic minerals including anatase grains. The diaspore bands are observed in the low-wavenumber region, namely between  $200\text{ cm}^{-1}$  and  $600\text{ cm}^{-1}$ . The most prominent are the  $705\text{ cm}^{-1}$ ,  $446\text{ cm}^{-1}$

**Table 1 – Summary of the XRD mineralogical analyses**

	<b>Sample</b>	<b>Description</b>	<b>Major Minerals</b>
<b>DIASPORIC</b>	ALM0306_PL1_B1 (3 <sup>rd</sup> horizon)	Red-brown to pale-brown, Massive	Diaspore, Hematite, Kaolinite
	ALM0306_PL1_B3 (3 <sup>rd</sup> horizon)	Red-brown, massive	Diaspore, Hematite, Anatase
	ALM0306_PL1_B4 (3 <sup>rd</sup> horizon)	Red-brown, slightly porous	Diaspore, Hematite, Goethite, Kaolinite
	ELM0206_DV_B1 (2 <sup>nd</sup> horizon)	Red-brown, massive	Diaspore, Anatase, Magnetite, Maghemite, Kaolinite
	SAB0306_ASV (3 <sup>rd</sup> horizon)	Red-brown, massive	Diaspore, Hematite, Anatase
	ALM0306_PL1_BS2 (3 <sup>rd</sup> horizon)	White-grey-yellow, highly porous	Diaspore, Anatase
	ALM0306_PL1_WB (3 <sup>rd</sup> horizon)	White-grey to pale-pink, highly porous	Diaspore, Anatase
	ELM0206_SK_B1a (3 <sup>rd</sup> horizon)	White-grey, highly porous	Diaspore, Anatase
	ELM0206_SK_B1b (3 <sup>rd</sup> horizon)	White-grey-yellow, highly porous	Diaspore, Anatase
	ALM0306_PL1_BIW (3 <sup>rd</sup> horizon)	White-grey, porous	Diaspore, Anatase
	ALM0306_BIW (3 <sup>rd</sup> horizon)	White-grey to pale-brown, highly porous	Diaspore, Anatase
	ELM0206_SK_B2 (3 <sup>rd</sup> horizon)	White-grey to yellow- brown, highly porous	Diaspore, Anatase, Goethite
	<b>BOEHMITIC</b>	ALM0306_PL1_B2 (3 <sup>rd</sup> horizon)	Red-brown, massive
ELM0206_KV_B1 (2 <sup>nd</sup> horizon)		Red-brown, massive	Boehmite, Hematite, Kaolinite
ELM0206_2H1 (2 <sup>nd</sup> horizon)		Red-brown-orange, massive	Boehmite, Goethite, Kaolinite
SAB0306_SKR (2 <sup>nd</sup> horizon)		Red-brown, massive	Boehmite, Hematite

and 260 cm<sup>-1</sup>, which are assigned to symmetric stretching modes (Ruan *et al.* 2001). In the porous white-grey bauxite samples the main diaspore band appears at 448 cm<sup>-1</sup> (solid arrow in Fig. 5), which is assigned to Al-O-Al stretching bend, and it is in good agreement with the results from the literature (Ruan *et al.* 2001, see Fig. 6). A number of strong peaks are also observed in the band

range between 1000 and 2000  $\text{cm}^{-1}$  which are attributed to fluorescence from the 633 nm He-Ne laser. Fluorescence peaks are wavelength-dependent and they should disappear when another laser is used, such as a Nd:YAG laser at 1064 nm. In synthetic diaspore a number of broad bands are observed with the 1064nm laser in the 2800-3700  $\text{cm}^{-1}$  region, attributed to the  $\nu(\text{OH})$  stretching. These bands were not observed in our spectra. The massive red-brown samples along with diaspore contain hematite (empty arrows in Fig. 5) with Raman bands at 612  $\text{cm}^{-1}$ , 496  $\text{cm}^{-1}$ , 412  $\text{cm}^{-1}$ , 293  $\text{cm}^{-1}$  and 225  $\text{cm}^{-1}$  (Faria *et al.* 1997, Bersani *et al.* 1999, Chamritski and Burns 2005, Zoppi *et al.* 2005, Zoppi *et al.* 2006).

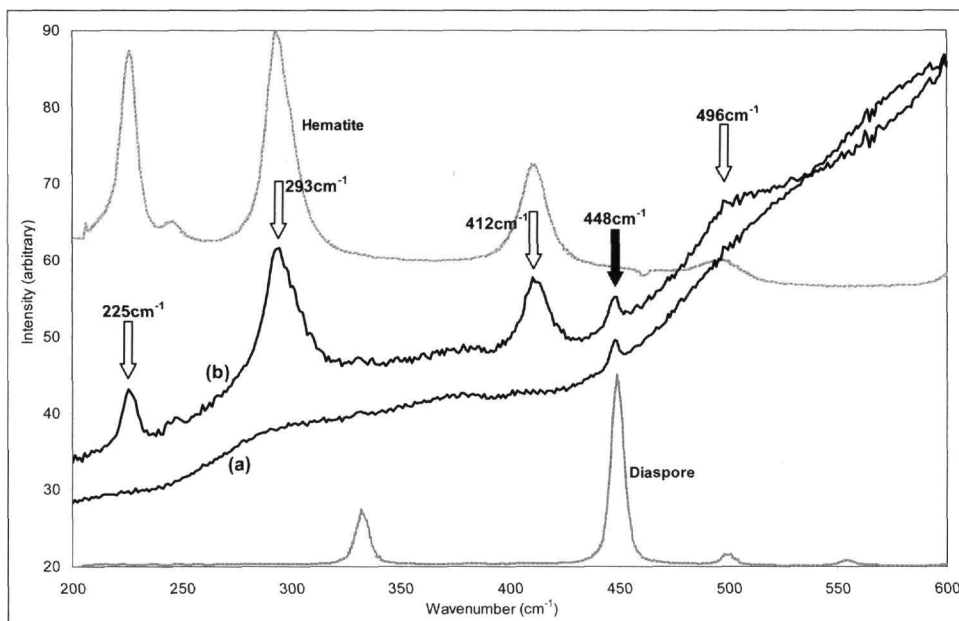


**Figure 5 – Representative Laser  $\mu$ -Raman spectra of diasporic bauxite samples in the low-wavenumber region (a: porous white-grey and b: massive red-brown). The lower spectrum corresponds to the Mineral Spectroscopy Server diaspore and the upper to standard hematite**

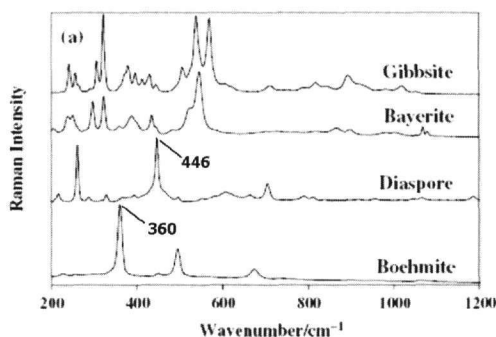


**Figure 6 – Raman spectra of different  $\text{AlOOH}$  polymorphs (Ruan *et al.* 2001). It is clearly marked the difference of the diasporic Raman band at 446  $\text{cm}^{-1}$  from the one of the boehmite at 360  $\text{cm}^{-1}$ , at the low-wavenumber region between 250  $\text{cm}^{-1}$  and 600  $\text{cm}^{-1}$**

Representative Laser  $\mu$ -Raman spectra of boehmitic bauxite samples (massive red-brown) are shown in Figure 7 (low-energy region). According to literature, the more intense boehmite peaks at the low-wavenumber region are at 674  $\text{cm}^{-1}$ , 495  $\text{cm}^{-1}$  and 360  $\text{cm}^{-1}$  and they correspond to the

hydroxyl translational modes. In our samples we observe the  $362\text{ cm}^{-1}$  band (Ruan *et al.* 2001, see Fig. 6). The spectrum (a) from Figure 7 corresponds to the boehmitic matrix of the sample, at an area where metallic minerals, such as rounded hematite aggregates were not optically visible. This band (solid arrow in Fig. 7) is observed between the  $412\text{ cm}^{-1}$  and  $293\text{ cm}^{-1}$  hematite bands and it could be used as a rule of thumb to easily distinguish it from the diasporic peak which is observed outside these hematite peaks (Faria *et al.* 1997, Bersani *et al.* 1999, Chamritski and Burns 2005, Zoppi *et al.* 2005, Zoppi *et al.* 2006).

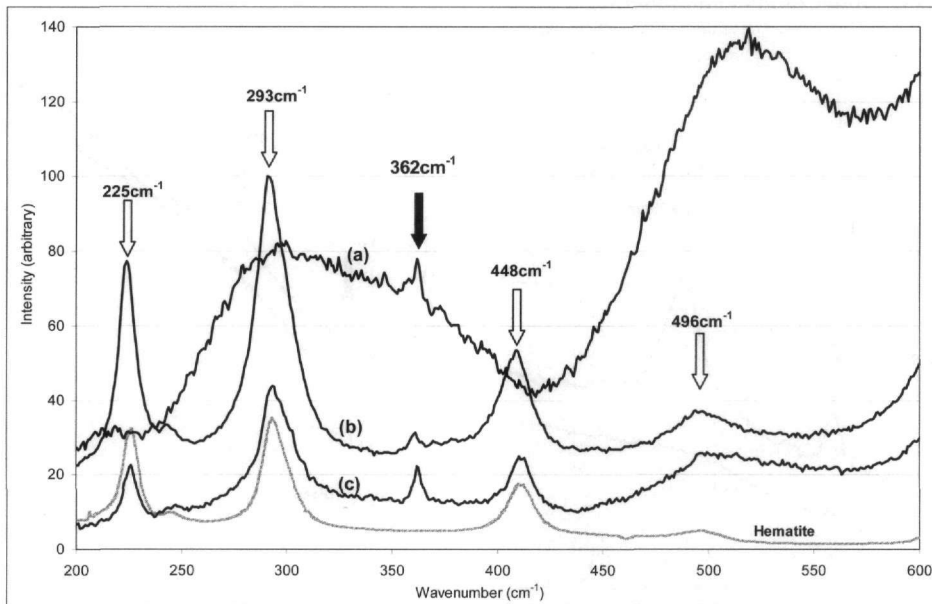


**Figure 7 – Representative Laser  $\mu$ -Raman spectra of boehmitic bauxite samples in the low-wavenumber region (a, b, c: massive red-brown). The lower spectrum corresponds to the Mineral Spectroscopy Server hematite**

At this point one could refer that the hematite Raman bands differ evidently to that of goethite, which may also be present in massive red-brown bauxites (either diasporic or boehmitic). In this case, the  $\text{AlOOH}$  polymorph bands (either at  $448\text{ cm}^{-1}$  or  $362\text{ cm}^{-1}$ ) are most probably expected to be distinguishable at the opposite sides of the main goethite band around  $385\text{ cm}^{-1}$  (Faria *et al.* 1997, Bersani *et al.* 1999). Furthermore, it is also expected that diasporic and boehmite low-wavenumber Raman bands will be apparent if kaolinite is present, under the laser beam spot, inasmuch the main –very intense– kaolinite band appears at  $140\text{ cm}^{-1}$  (Johnston *et al.* 1984, Frost *et al.* 1993).

**Table 2 – Summary of the Laser  $\mu$ -Raman data**

	Raman bands ( $\text{cm}^{-1}$ )	
	<b>AlOOH polymorphs</b>	<b>Hematite (<math>\alpha\text{-Fe}_2\text{O}_3</math>)</b>
<b>Diasporic Type</b>		
White-grey bauxites	448	-
Red-brown bauxites	448	412, 293, 225
<b>Boehmitic Type</b>		
Red-brown bauxites	362	612, 412, 293, 225

Concluding, the results of the present study suggest that Laser  $\mu$ -Raman spectroscopy could be applied for the fast determination of the AlOOH polymorphs and, as a consequence, the “type” of bauxite of the Parnassos-Ghiona active mining area (central Greece). In the case of the white-grey (high-quality) diasporic bauxite there is a clear diasporic Raman band at  $448\text{ cm}^{-1}$  to be used as the characteristic band, while in the case of the typical red-brown diasporic bauxite the same band is accompanied by the unavoidable bands of hematite (Table 2). For the red-brown boehmitic bauxite, the main Raman band of boehmite appears at  $362\text{ cm}^{-1}$ , between two major hematite bands. It is therefore demonstrated that both diasporic and boehmitic bauxites can easily be characterized by recording Raman spectra in the  $250\text{ cm}^{-1} - 600\text{ cm}^{-1}$  region. In this low-wavenumber region the bands of the AlOOH polymorphs do not interfere with bands from other bauxite minerals. A portable Raman system with a CCD acquisition camera and with a laser operating at the wavelength of  $1064\text{ nm}$  could be used to rapidly acquire the narrow spectra range between  $250\text{ cm}^{-1}$  and  $600\text{ cm}^{-1}$ . The He-Ne laser with a wavelength of  $633\text{ nm}$  introduces significant fluorescence which might suppress the Raman peaks and make them invisible. However, it still can be used when the CCD is centred to cover the low wavenumber region but it may require longer integration times. The use of a powder XRD or of another time-consuming technique is not necessary in order to distinguish the type of bauxite (diasporic or boehmitic). This could be particularly useful in characterising similar in appearance samples such as the massive red-brown samples (e.g. SAB0306\_ASV and SAB0306\_SKR, see Table 1) which could be of diasporic or boehmitic type. Future work could employ direct tests on site with a portable Raman system that has the above characteristics. Furthermore, one could proceed into calibrating a portable system to acquire quantitative or semi-quantitative information for precise quality assessment during production.

#### 4. Acknowledgments

We would like to thank the Greek bauxite mining companies (Aluminium de Grèce S.A., S&B Industrial Minerals S.A. and Elmin S.A.) for their kindly help concerning underground visits and supply of samples from their Parnassos-Ghiona mines.

#### 5. References

- Aronis, G. A., 1955. Geographical distribution, geological placing and aspects on the genesis of the Greek bauxites, *Bull. Geol. Soc. Greece*, 2, 55-79.
- Arp, T., 1985. Geologische Kartierung des Gebietes um Tithronion im Kallidromengebirge, Mittelgriechenland und petrographische Bearbeitung des Karstbauxites (b1), *PhD Thesis*, Univ. of Hamburg, Hamburg, 213pp. (unpublished)
- Augustithis, S.S., Mack, E., and Vgenopoulos, A., 1978. Textural and geochemical comparisons of the oolitic and pisolitic structures of the Parnassus Bauxites and the Ni-Cr-Fe Laterites of Larymna/Lokris and Euboea, Greece, *4th International Congress for the Study of Bauxites, Alumina and Aluminum*, Athens. October 9-12, 15-34pp.
- Bárdossy, Gy., 1982. *Karst Bauxites. Bauxite Deposits on Carbonate Rocks*, Elsevier, 441pp.
- Bárdossy, Gy., and Mack, E., 1967. Zur Kenntnis der Bauxite des Parnass-Kiona-Gebirges, *Mineralium Deposita*, 2, 334-348.
- Bárdossy, Gy., and Pantó, Gy., 1971. Investigation of Bauxites with Help of Electron-Probe, *TMPM Tschermarks Min. Petr. Mitt.*, 15, 165-184.
- Bersani, D., Lottici, P.P., and Montenero, A., 1999. Micro-Raman Investigation of Iron Oxides Films and Powders Produced by Sol-Gel Syntheses, *J. Raman Spectrosc.*, 30, 355-360.



- Biermann, M., 1983. Zur Mineralogie, Geochemie und Genese des Karstbauxites (B3-Horizont) an der Grenze Unter- Oberkreide in Mittelgriechenland, *PhD Thesis*, Univ. of Hamburg, Hamburg, 134 pp.
- Chamritski, I., and Burns, G., 2005. Infrared and Raman-Active Phonons of Magnetite, Maghemite and Hematite: A Computer Simulation and Spectroscopic Study, *J. Phys. Chem.*, 109, 4965-4968.
- Combes, P.J., 1979. Observations sédimentologiques, paléogéographiques, minéralogiques et géochimiques sur les bauxites du deuxième horizon dans la zone du Parnasse (Grèce), *Bull. Soc. Géol. Fr.*, (7), XXI, 4, 485-494.
- Combes, P.J., and Andreou, G., 1983. Utilisation de la paléogéographie pour la prospection de bauxite dans une région de nappe: un exemple au nord de Distomon (zone du Parnasse, Grèce), *5th Int. Congress ICSOBA*, Zagreb, 223-231.
- Combes, P.J., Fourcade, E., Masse, J.P., and Philip, J., 1981. Observations stratigraphiques et paléontologiques sur la Crétacé de la zone du Parnasse, *Trav. Comité Int. Etude des Bauxites, de l'Alumine et de Aluminium*, *Acad. Yougoslav. Sci. Arts*, 11 (16), 347-365.
- Economopoulos, I.E., and Vgenopoulos, A.G., 1998. An approach concerning bauxites, bauxitization and mining in Greece, *Mineral Wealth*, 109, 21-34. (in English, with Greek abstract)
- Economopoulou-Kyriakopoulou, N., 1991. A comparative geochemical and mineralogical study of bauxitic horizons in central Greece, *PhD Thesis*, National Technical University of Athens, Faculty of Mining Engineering and Metallurgy. Athens, 119pp. (unpublished)
- Faria, D.L.A., Venâncio Silva, S., and Oliveira, M.T., 1997. Raman Microspectroscopy of Some Iron Oxides and Oxyhydroxides, *J Raman Spectrosc.*, 28, 873-878.
- Frost, R.L., Fredericks, P.M., and Bartlett, J.R., 1993. Fourier transform Raman spectroscopy of kandite clays, *Spectrochimica Acta*, 49A (5/6), 667-674.
- Johnston, C.T., Sposito, G., Bocian, D.F., and Birge, R.R., 1984. Vibrational spectroscopic study of the interlamellar kaolinite-dimethyl sulfoxide complex, *Journal of Physical Chemistry*, 88, 5959-5964.
- Kiskyras, D., 1960. Die mineralogische Zusammensetzung der griechischen Bauxite in Abhängigkeit von der Tektonik, *Neues Jahrb. Mineral. Abhandl.*, 94, 662-680.
- Kritsotakis, K., Schulz-Dobrick, B., and Panagos, A.G., 1986. REE-Mineralen in Griechischen Bauxiten, *Fortschritte der Mineralogie, Beiheft*, 64 (1), 87.
- Laskou, M., 1991. Concentrations of rare earths in Greek Bauxites, *Acta Geologica Hungarica*, 34 (4), 395-404.
- Laskou, M., 2001. Chromite in karst bauxites, bauxitic laterites and bauxitic clays of Greece. In Piestrzynski, et al. (eds), *Mineral Deposits at the Beginning of the 21st century*, 6th Biennial SGA Meeting, Krakow. Millpress, Rotterdam, 1091-1094pp.
- Laskou, M., 2005. Pyrite-rich bauxites from the Parnassos-Ghiona zone, Greece. In Mao, et al. (eds), 8th SGA Meeting, "Mineral Deposits Research Meeting the Global Challenge" Beijing, August 18-21, 1007-1010pp.
- Laskou, M., and Andreou, G., 2003. Rare earth element distribution and REE-minerals from the Parnassos-Ghiona bauxite deposits, Greece. In D. Eliopoulos, et al. (eds), *Mineral Exploration and Sustainable Development*, 7th Biennial SGA Meeting, Athens. Millpress, Rotterdam, 89-92pp.

- Laskou, M., and Economou, M., 1991. Platinum group elements and gold concentrations in Greek bauxites, *Geologica Balcanica*, 21 (2), 65-77.
- Laskou, M., and Economou, M., 2006. The role of microorganisms on the mineralogical and geochemical characteristics of the Parnassos-Ghiona bauxite deposits, Greece, *Journal of Geochemical Exploration*. (in press)
- Lymperopoulou, Th., 1996. Determination and extraction of rare earth elements from bauxites and red mud, *PhD Thesis*, National Technical University of Athens, Faculty of Chemical Engineering, Athens, 183pp. (unpublished)
- Mack, E., and Petrascheck, W.E., 1978. Palaeogeographie, Verteilung und Qualität der Bauxite im Parnass-Kjona Gebirge, 4. *Intern. Congr. ICSOBA*, 2, 526-539.
- Maksimović, Z., and Papastamatiou, J., 1973. Distribution d'oligoéléments dans les gisements de bauxite de la Grèce centrale, *Symp. ICSOBA*, Nice, 33-46.
- Nia, R., 1968. Geologische und petrographische Untersuchungen zum Problem der Boehmit-Diaspor-Genese in griechischen Oberkreide-Bauxiten der Parnass-Kiona-Zone, *PhD Thesis*, Univ. of Hamburg, Hamburg, 133pp.
- Nia, R., 1968. Zur Bedeutung der methodischen Probenahme für genetische Untersuchungen von Bauxit-Lagerstätten am Beispiel der Oberkreide-Bauxite der Parnass-Kiona-Zone Griechenlands, *Mineralium Deposita*, 3, 368-374.
- Nia, R., 1971. Genesis of boehmite and diaspor in Greek Upper Cretaceous bauxites of the Parnasse-Gjona zone, *Proc. 2<sup>nd</sup> Int. Syrup. ICSOBA*, Budapest, 69-98.
- Nicolas, J., and Bildgen, P., 1979. Relations between the location of the karst bauxites in the northern hemisphere, the global tectonics and the climatic variations during geological time, *Palaeogeography, Palaeoclimatology, Palaeoecology*, 28, 205-239.
- Ochsenkühn, K.M., Fafouteli, P., and Ochsenkühn-Petropoulou, M., 2002. Determination and distribution of gold in Greek Bauxites of the Parnassos-Gkiona area by gamma-spectroscopy after ion exchange separation, *Journal of Radioanalytical and Nuclear Chemistry*, 253(2), 257-262.
- Ochsenkühn, K.M., Ochsenkühn-Petropoulou, M., and Parissakis, G., 1995. Activation analysis of bauxitic materials by epithermal irradiation, *Journal of Radioanalytical and Nuclear Chemistry*, 190 (1), 75-79.
- Ochsenkühn, K.M., and Parissakis, G., 1977. Quantitative Untersuchungen von Bauxiten Zentralgriechenlands mittels Atomabsorptions-spectroscopie und Flemmenatomemission, *Microchimica Acta*, 1, 447-457.
- Ochsenkühn-Petropoulou, M., and Ochsenkühn, K.M., 1995. Comparison of inductively coupled plasma mass spectrometry with inductively coupled plasma atomic emission spectrometry and instrumental neutron activation analysis for the determination of rare earth elements in Greek bauxites, *Spectrochimica Acta*, 46 (1), 51-65.
- Ochsenkühn-Petropoulou, M., and Ochsenkühn, K.M., 1995. Rare earth minerals found in Greek Bauxites by SEM and EPMA, *European microscopy and analysis*, September 1995, 13-14.
- Papastamatiou, J., 1960. La géologie de la région montagneuse du Parnass-Kiona-Oeta, *Bull. Géol. Soc. Fr.*, 7, 398-409.
- Papastamatiou, J., 1964. Les gisements de bauxite en Grèce, *1st Symp. ICSOBA*, Zagreb, 285-293.

- Papastavrou, S., 1974. Einige Bemerkungen zur Relation zwischen Verkarstungsbahnen und Längserstreckung der Bauxitlager bei Sideroporto-Bela, *Ann. Fac. Phys. — Math, Univ.*, 1–99.
- Papastavrou, S., 1986. Greek bauxites (Description – Classification – Distribution – Problems), Mineral Deposits Research. IGME, Internal Report. Athens, 30pp. (in Greek, with English abstract)
- Papastavrou, S., and Perdikatsis, V., 1987. U-Th and REE concentrations in bauxites and new aspects about the origin of bauxites in the mountains, *Mineral Deposits of the Tethyan Eurasian Belt*, ed. S. Janković, Faculty of Mining, Belgrade.
- Paspaliaris, J., 1985. A contribution to the optimization of diasporic bauxite leaching process, *PhD Thesis*, National Technical University of Athens, Faculty of Mining Engineering and Metallurgy, Athens, 185pp. (unpublished)
- Perdikatsis, V., 1992. Quantitative mineralogical analysis of bauxites by X-ray diffraction with the Rietveld method, *Acta Geologica Hungarica*, 35 (4), 447-457.
- Petrascheck, W.E., 1989. The genesis of allochthonous karst-type bauxite deposits of southern Europe, *Mineralium Deposita*, 24, 77-81.
- Ruan, H.D., Frost, R.L., and Kloprogge, J.T., 2001. Comparison of Raman spectra in characterizing gibbsite, bayerite, diaspore and boehmite, *J. Raman Spectrosc.*, 32, 745-750.
- Solymár, K., Mádai, F., and Papanastasiou, D., 2005. Effect of bauxite microstructure on beneficiation and processing, *Light Metals 2005* Edited by Halvor Kvande TMS (The Minerals, Metals & Materials Society), 47-52pp.
- Valeton, I., 1972. *Bauxites. Development in Soil Sciences*, 1, Elsevier, 226pp.
- Valeton, I., 1991. Processes of allochthony and autochthony in bauxites on carbonate platforms of the Mediterranean Area, *Mineral Wealth*, 71, 13-28.
- Valeton, I., Biermann, M., Reche, R., and Rosenberg, F., 1987. Genesis of nickel laterites and bauxites in Greece during the Jurassic and the Cretaceous and their relation to ultrabasic rocks, *Ore Geology Reviews*, 2, 359–404.
- Vgenopoulos, A., and Daskalakis, K., 1991. Remarks on the genesis and ore-dressing of the alluvial bauxite occurrences of Parnassos-Gkiona-Elikon, *Acta Geologica Hungarica*, 34 (4), 405-407.
- Zoppi, A., Lofrumento, C., Castellucci, E.M., Dejoie, C., and Sciau, Ph., 2006. Micro-Raman study of aluminium-bearing hematite from slip of Gaul *sigillata* wares, *J. Raman Spectrosc.*, 37, 1131-1138.
- Zoppi, A., Lofrumento, C., Castellucci, E.M., and Migliorini, M.G., 2005. The Raman spectrum of hematite: Possible indicator for a compositional or firing distinction among *terra sigillata* wares, *Annali di Chimica*, 95, 239-246.